

# Model-based estimation and control of particle velocity and melting in HVOF thermal spray

Mingheng Li, Dan Shi, Panagiotis D. Christofides\*

*Department of Chemical Engineering, University of California, Los Angeles, CA 90095-1592, USA*

Received 24 February 2004; received in revised form 15 June 2004; accepted 11 July 2004

Available online 15 September 2004

## Abstract

This work focuses on the development of model-based estimation and control algorithms for regulating particle velocity and degree of melting in the high velocity oxygen fuel (HVOF) thermal spray process. Initially, an estimation scheme, which is based on gas phase measurements and the particle velocity and temperature equations, is proposed to estimate the volume-based average of particle velocity and melting degree at the point of impact on the substrate. Then, a feedback control system, which directly uses the estimation scheme, is designed to regulate the volume-based average of the particle velocity and degree of melting by manipulating the inlet gas flow rates to the process. The proposed estimation/control structure is applied to a fundamental model of the industrial Diamond Jet hybrid HVOF thermal spray process and its performance and robustness properties are tested through simulations.

© 2004 Elsevier Ltd. All rights reserved.

*Keywords:* HVOF thermal spray; Coatings; Estimation; Control

## 1. Introduction

The high velocity oxygen-fuel (HVOF) thermal spray process is a process of particulate deposition in which fine powder particles, normally in the size range 5–65  $\mu\text{m}$ , are heated and accelerated in a reacting gas stream and subsequently hit a substrate in a molten or semi-molten state, forming a thin layer of coating as a result of the solidification and sintering of the sprayed particles. Featured with very high particle velocities and relatively low particle temperatures as compared to those in the plasma spray process, the HVOF thermal spray provides a highly efficient way to coating processing in order to extend product life, increase performance and reduce production and maintenance costs. Nowadays, the HVOF thermal spray has carved out a special niche in the thermal spray industry, particularly in the

fabrication of nano-structured coatings, because the particle vaporization or overheating is avoided during flight and the nano-crystalline structure of powder particles can be preserved (Cheng et al., 2003).

Generally speaking, the physical properties of a thermally sprayed coating are strongly influenced by the microstructure of the deposit, which, in turn, depends to a large extent on the physical and chemical state of particles at the point of impact on the substrate, such as velocity, temperature, degree of melting and oxidant content. These variables, however, are strongly dependent on several key process parameters including the fuel/oxygen ratio, total gas flow rate, spray distance and powder size distribution (Li et al., 2004a). Despite significant experimental (Lugscheider et al., 1998; Hearley et al., 2000; Moreau and Leblanc, 2001) and theoretical (Cheng et al., 2001a,b; Li and Christofides, 2003; Shi et al., 2004) studies exploring the relationship between key process parameters and particle characteristics at impact and the resulting coating thermal and mechanical properties, the development and implementation of feedback control

\* Corresponding author. Tel.: +1-310-794-1015; fax: +1-310-206-4107.  
E-mail address: [pdchristofides@seas.ucla.edu](mailto:pdchristofides@seas.ucla.edu) (P.D. Christofides).

systems on HVOF thermal spray processes, which will allow the fabrication of coatings with low variability and high performance, remains a challenging task in the thermal spray industry.

Motivated by the above, in our previous work (Li et al., 2004a; Shi et al., 2004), we performed a comprehensive control-relevant parametric analysis of the industrial Diamond Jet hybrid HVOF thermal spray and proposed a feedback control system targeting the control of volume-based average of particle velocity and melting degree at the point of impact on the substrate by manipulating the feeding gas flow rates. Our previous work was based on the assumption of availability of particle velocity and temperature measurements. In practice, it is difficult to directly measure the degree of melting of individual particles and consequently, the average degree of melting of the entire particle size distribution. To overcome this limitation, in the present paper, we propose an estimation scheme to obtain real-time estimates of particle velocity, temperature and degree of melting. The proposed estimation scheme is based on the modeling equations which describe the evolution of particle temperature, velocity and degree of melting coupled with the available gas phase measurements. Then, a feedback control system, which directly uses the estimation scheme, is designed to regulate the volume-based average of the particle velocity and degree of melting by manipulating the inlet gas flow rates to the process. The proposed estimation/control structure is applied to a fundamental model of the industrial HVOF thermal spray process and its performance and robustness properties are tested through simulations.

**2. Diamond jet hybrid HVOF thermal spray: description and modeling**

Fig. 1 shows a schematic diagram of the Diamond Jet hybrid HVOF thermal spray gun, which is currently used in industry. There are three major physicochemical processes involved in this process: transformation of chemical energy into thermal energy by the combustion of the fuel,

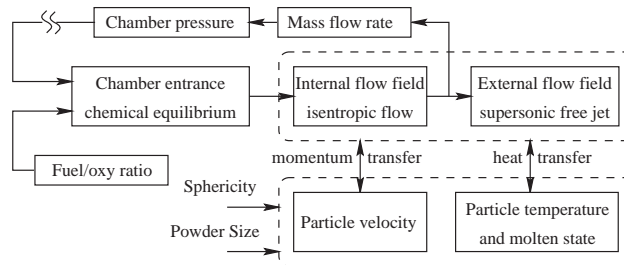


Fig. 2. Modeling procedure of the gas and particle field.

conversion of thermal energy into kinetic energy of the burning gases by passing through the convergent–divergent nozzle, and transfer of momentum and heat from the gas to the powder particles. The flow and thermal characteristics of the process can be described either by a comprehensive CFD model(Li and Christofides, 2004) or by a simplified one-dimensional model (Li et al., 2004a), depending on the process features to be incorporated and computational cost required. To make the solution time of the HVOF thermal spray process model comparable to the real-time process evolution, the latter is used here. Specifically, the model is based on the one-way coupling assumption of the gas phase and the particulate phase because of very small particle loading, and these two phases are solved by Eulerian and Lagrangian approaches, respectively (see Fig. 2). On the gas dynamics side, it is assumed that most of the reaction occurs in the combustion chamber (convergent part of the nozzle) and the reaction moves forward following an equilibrium chemistry model (Swank et al., 1994) based on the fact that the residence time of gas in the combustion chamber is much longer than the subsequent parts. The heat released from the exothermic reaction increases the gas temperature to slightly higher than 3100 K and a high pressure of 6 atm is maintained in the combustion chamber. During passage through the nozzle, the thermal energy is partially converted to kinetic energy. If the effects of water-cooling and friction on the wall can be ignored, several relationships can be derived from the governing mass, momentum and energy conservation

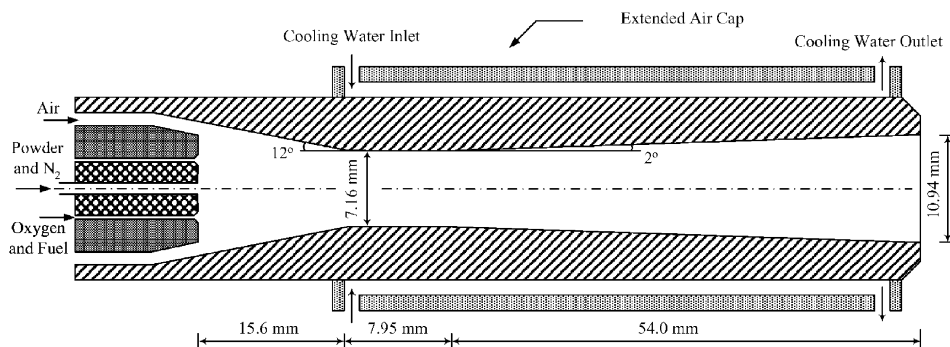


Fig. 1. Schematic diagram of the Diamond Jet hybrid thermal spray gun.

equations to relate the gas properties between two positions in the nozzle (Roberson and Crowe, 1997):

$$\frac{A_2}{A_1} = \frac{M_1}{M_2} \left\{ \frac{1 + [(\gamma - 1)/2]M_2^2}{1 + [(\gamma - 1)/2]M_1^2} \right\}^{(\gamma+1)/2(\gamma-1)}, \quad (1)$$

$$\frac{T_2}{T_1} = \frac{1 + [(\gamma - 1)/2]M_1^2}{1 + [(\gamma - 1)/2]M_2^2}, \quad (2)$$

$$\frac{P_2}{P_1} = \left\{ \frac{1 + [(\gamma - 1)/2]M_1^2}{1 + [(\gamma - 1)/2]M_2^2} \right\}^{\gamma/(\gamma-1)}, \quad (3)$$

$$\frac{\rho_2}{\rho_1} = \left\{ \frac{1 + [(\gamma - 1)/2]M_1^2}{1 + [(\gamma - 1)/2]M_2^2} \right\}^{1/(\gamma-1)}, \quad (4)$$

where  $A$  is the cross-sectional area perpendicular to the flow direction,  $T$  is the gas temperature,  $\rho$  is the gas density,  $P$  is the pressure,  $\gamma$  is the specific heat ratio, and  $M$  is the mach number defined as the ratio of gas velocity to the local sonic velocity ( $a = \sqrt{\gamma P/\rho}$ ). Since the flow is choked at the throat area, where the mach number is 1, the mass flow rate at the throat of the nozzle is given by  $A_t \rho_t a_t$  (subscript  $t$  denotes throat), which should match the specified mass flow rate at the entrance of the torch. Based on this, an iterative procedure is used to determine the combustion pressure. The reader may refer to (Li et al., 2004a) for details on the solution method. Once the gas properties at a specific point are determined, the entire internal flow/thermal field will be readily solved using Eqs. (1–4). Regarding the supersonic free jet in the external flow field, since the capture of shock diamonds using a one-dimensional model is very difficult, it is modeled by taking advantage of the experimentally measured data available for supersonic free jets (Li et al., 2004b):

$$\overline{gP} = 1 - \exp\left(\frac{\alpha}{1 - \bar{x}/\beta}\right), \quad (5)$$

where  $\overline{gP}$  refers to normalized gas properties ( $v/v_e$ ,  $(T - T_a)/(T_e - T_a)$  and  $(\rho - \rho_a)/(\rho_e - \rho_a)$ , where the subscripts  $a$  and  $e$  stand for atmospheric condition and nozzle exit condition, respectively),  $\bar{x}$  is the normalized axial distance from the exit of the nozzle ( $\bar{x} = x/D$ , where  $D$  is the diameter of the nozzle exit) and  $\alpha$ ,  $\beta$  are constants.

On the particle dynamics side, under the assumptions of (1) negligible particle coagulation during flight due to small particle loading (or the powder size does not change during flight; the control of powder size distribution due to nucleation condensation and coagulation etc. in aerosol processes can be found in (Kalani and Christofides, 1999, 2000, 2002)), (2) particle motion primarily due to drag force (other forces, such as gravitational force, Magnus force, and force due to pressure gradient etc. are not included), (3) negligible internal resistance of particle heating, and (4) weak dependence of particle heat capacity on temperature, the particle trajectories and temperature histories in the gas field can be computed

by the following equations:

$$m_p \frac{dv_p}{dt} = \frac{1}{2} C_D \rho_g A_p (v_g - v_p) |v_g - v_p|, \quad v_p(0) = v_{p0}, \quad (6)$$

$$\frac{dx_p}{dt} = v_p, \quad x_p(0) = 0, \quad (7)$$

$$m_p c_{pp} \frac{dT_p}{dt} = \begin{cases} hA'_p(T_g - T_p) + S_h, & (T_p \neq T_m) \\ 0, & (T_p = T_m) \end{cases} \quad (8)$$

$$\Delta H_m m_p \frac{df_p}{dt} = \begin{cases} hA'_p(T_g - T_p) + S_h, & (T_p = T_m) \\ 0, & (T_p \neq T_m) \end{cases} \quad (9)$$

where  $m_p$  is the mass of the particle,  $t$  is the time,  $v_p$  is the axial velocity of the particle,  $A_p$  is the projected area of the particle on the plane perpendicular to the flow direction,  $\rho_g$  is the density of the gas,  $C_D$  is the drag coefficient (function of the local Reynolds number and sphericity),  $x_p$  is the position of the particle,  $T_p$  is the temperature of the particle,  $A'_p$  is the surface area of the particle,  $T_m$  is the melting point of the particle,  $\Delta H_m$  is the enthalpy of melting,  $f_p$  is the mass fraction of melted part in the particle ( $0 \leq f_p \leq 1$ ) and  $S_h$  is a source term including heat transfer due to radiation ( $\epsilon \sigma A'_p (T_g^4 - T_p^4)$ ) and oxidation. The above equations describing particle velocity, position, temperature and degree of particle melting are solved by the 4th order Runge-Kutta method. The thermodynamic and transport properties of the mixture are calculated using the formulas provided in (Gordon and McBride, 1994). Note that in the HVOF thermal spray processing of particles consisting of carbides with binding metals, such as the WC-Co powders used in this work, only the latter may experience a molten state because the gas temperature in a conventional HVOF thermal spray process is not high enough to melt the carbides, whose melting point is very high (i.e. 2870 °C for tungsten carbide) (Sobolev et al., 1994). In such a case, the particle melting equation in Eq. (9) is modified such that only the fusion of metals might occur in the gas thermal field. In the present work, the melting degree of particles represents the one of the binder (Cobalt) instead of the whole particulate phase. The simulation studies show that particles of different sizes are not uniformly accelerated (or decelerated) and heated (or cooled) in the gas flow/thermal field due to different momentum and thermal inertias. Small particles, which have small momentum and thermal inertias, are prone to change their velocities and temperatures. Big ones, however, are difficult to be accelerated (or heated) or decelerated (or cooled). The interplay between the nonuniform distribution of particle momentum and thermal inertias and the decay of gas velocity and temperature in the free jet results in the fact that particles in the moderate size range usually attain higher velocities and melting degrees than both larger and smaller ones as they arrive at the substrate. In particular, particles of different sizes might have different molten states, i.e., particles of moderate sizes may be fully melted or partially

melted at the point of impact on the substrate, and particles of either small or large sizes are usually not melted as they hit the substrate (Li et al., 2004a). The nonuniform molten states of particles of different sizes drawn from model predictions are supported by experimental observations (He et al., 2001; Zhang et al., 2003).

### 3. Real-time estimation of volume-averaged particle velocity and melting ratio

The velocity, temperature and melting degree of particles at the point of impact on the substrate are two key parameters that determine the coating thermal and mechanical properties. In particular, our previous work based on stochastic simulation of coating microstructure (Shi et al., 2004) as well as experimental investigations of other groups (Moreau and Leblanc, 2001) have shown that a high degree of particle melting improves powder deposition efficiency and decreases coating porosity. We note that the powders used in the HVOF thermal spray process are usually polydisperse, and the larger the particle is, the more it contributes to the coating properties. In this sense, the volume-based averages of particle velocity and melting degree constitute better choices of controlled outputs than the number-based ones. At this point, it is important to note that a calculation of the volume-based particle properties requires an explicit relationship between the particle velocity, temperature, melting ratio and the particle size, i.e.

$$\overline{pp} = \frac{\int_0^\infty \frac{1}{6} \pi d_p^3 pp(d_p) f(d_p) d(d_p)}{\int_0^\infty \frac{1}{6} \pi d_p^3 f(d_p) d(d_p)}, \quad (10)$$

where  $pp$  stands for particle properties,  $d_p$  is the particle size and  $f(d_p)$  is the powder size distribution function. The size distribution of most powders can be adequately described by lognormal functions of the following form (Li and Christofides, 2003, 2004):

$$f(d_p) = \frac{1}{\sqrt{2\pi}\sigma d_p} \exp\left[-\frac{(\ln d_p - \mu)^2}{2\sigma^2}\right], \quad (11)$$

where  $\mu$  and  $\sigma^2$  are two dimensionless parameters corresponding to the mean and the variance of  $\ln d_p$ , which obeys Gaussian distribution. However, most of the online measurements, including particle size, velocity and temperature using Laser Doppler Velocimeter, Two Color Pyrometer, etc. (Fincke et al., 1990; Knight et al., 1994; Fincke et al., 2001) can only give histogram counts properties and the relationship between particle velocity, temperature and particle size is implicit. Moreover, it is very difficult to directly measure the degree of melting of individual particles and consequently, the average degree of melting of the entire particle size distribution. To overcome this limitation, one needs to use an estimation scheme based on the modeling equations

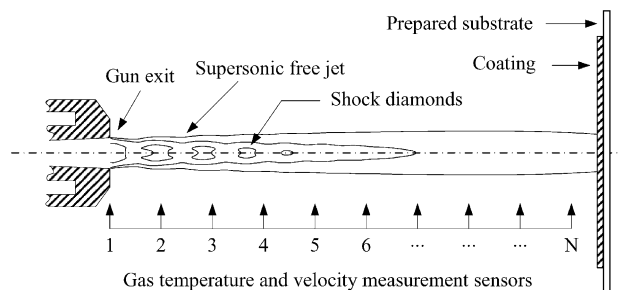


Fig. 3. Diagram of the gas phase measurement system.

that describe the evolution of particle temperature, velocity and degree of particle melting coupled with the available gas phase measurements to estimate average particle melting ratio and velocity at the point of impact on the substrate.

In an industrial environment, where the presence of measurement noise is not negligible, it is desirable to estimate the states of the system with as little uncertainty as possible in the presence of noise. This entails the implementation of a real-time estimator to alleviate the effect of measurement noise. In the present work, it is assumed that the gas velocity and temperature are measured by  $N$  Rayleigh scattering based sensors placed downstream of the gun exit (Fig. 3). To account for measurement noise, the measured gas velocity and temperature at various locations in the free jets are described by:

$$\begin{aligned} v'_g(x_i) &= \bar{v}_g(x_i) + R_v, \\ T'_g(x_i) &= \bar{T}_g(x_i) + R_T, \end{aligned} \quad (12)$$

where  $\bar{v}_g(x_i)$  and  $\bar{T}_g(x_i)$  are the model predicted gas velocity and temperature at the  $i$ th location, and  $v'_g(x_i)$  and  $T'_g(x_i)$  are the corresponding measured values.  $R_v$  and  $R_T$  are two independent random numbers which obey Gaussian distribution. In the computer simulation, both of them are assumed to have a zero mean and a variance of  $150^2$ . An adaptive filter is used in this paper to reject the stochastic fluctuations contained in the gas phase measurements. Specifically, the adaptive filter is a second-order dynamical system with the following representation:

$$\begin{aligned} \frac{d\hat{y}_i}{dt} &= \xi_i, \\ \frac{d\hat{\xi}_i}{dt} &= \frac{K_i}{\tau_i} (y_i - \hat{y}_i) - \frac{1}{\tau_i} \hat{\xi}_i, \end{aligned} \quad (13)$$

where  $y_i$  is the gas velocity (or temperature) measurements at the  $i$ th location,  $\hat{y}_i$  is the corresponding filter output,  $K_i$  is the filter gain and  $\tau_i$  is the filter time constant. To accelerate the response of the filter and avoid large overshoot,  $\tau$  is set to be  $0.5/K$ . The filter gain is adaptively adjusted according to the following law:

$$K(t) = K_0 \frac{|\int_{t-\Delta t}^t y(t) dt - \int_{t-2\Delta t}^{t-\Delta t} y(t) dt|}{\Delta t^2} + K_s \quad (14)$$

to achieve both fast tracking of the dynamics of the outputs and efficient noise rejection, where  $K_0$  is a constant,  $K_s$  is the steady-state gain for the adaptive filter and  $\Delta t$  is the time interval between two updates of  $K$ .

Interpolation is applied to the set of gas phase measurements ( $v_g(x_i)$  and  $T_g(x_i)$ ) to determine the profiles of gas velocity and temperature across  $x$ . For instance, the gas properties at position  $x_p$  can be calculated as the weighted sum of the measured values as follows:

$$\begin{aligned} \hat{v}_g(x_p) &= \sum_{i=1}^N \alpha(i) \hat{v}_g(x_i), \\ \hat{T}_g(x_p) &= \sum_{i=1}^N \beta(i) \hat{T}_g(x_i), \end{aligned} \quad (15)$$

where  $\alpha(i)$  and  $\beta(i)$  are coefficients that can be determined using standard techniques, for example, the Lagrangian interpolation method (Press et al., 1997). Using the expression of gas velocity and temperature of Eq. (15), we can construct the following equations:

$$\begin{aligned} m_p \frac{d\hat{v}_p}{dt} &= \frac{1}{2} C_D \rho_g A_p \left( \sum_{i=1}^N \alpha(i) \hat{v}_g(x_i) - \hat{v}_p \right) \\ &\quad \times \left| \sum_{i=1}^N \alpha(i) \hat{v}_g(x_i) - \hat{v}_p \right|, \hat{v}_p(0) = v_{p0} \\ \frac{d\hat{x}_p}{dt} &= \hat{v}_p, \hat{x}_p(0) = 0 \\ m_p c_{pp} \frac{d\hat{T}_p}{dt} &= h A'_p \left( \sum_{i=1}^N \beta(i) \hat{T}_g(x_i) - \hat{T}_p \right) \\ &\quad + S_h, (\hat{T}_p \neq T_m), \hat{x}_p = T_{p0} \\ \Delta H_m m_p \frac{d\hat{f}_p}{dt} &= h A'_p \left( \sum_{i=1}^N \beta(i) \hat{T}_g(x_i) - \hat{T}_p \right) \\ &\quad + S_h, (\hat{T}_p = T_m), \hat{f}_{p0} = 0 \end{aligned} \quad (16)$$

from which the estimates of velocity, temperature and melting degree of each individual particle in the whole gas flow/thermal field can be obtained. The estimated average particle properties are then readily calculated using Eq. (10).

Fig. 4 shows the estimates of particle velocity and melting ratio, obtained with (dashed line) and without (solid line) the use of filtering of the gas velocity and temperature measurements. Clearly, the filter is quite effective in alleviating the effect of the measurement noise on the estimates of particle velocity and degree of melting.

#### 4. Model-based feedback control of particle velocity and melting degree

To formulate the control problem, we follow the strategy proposed in Li et al. (2004a). Specifically, the volume-based

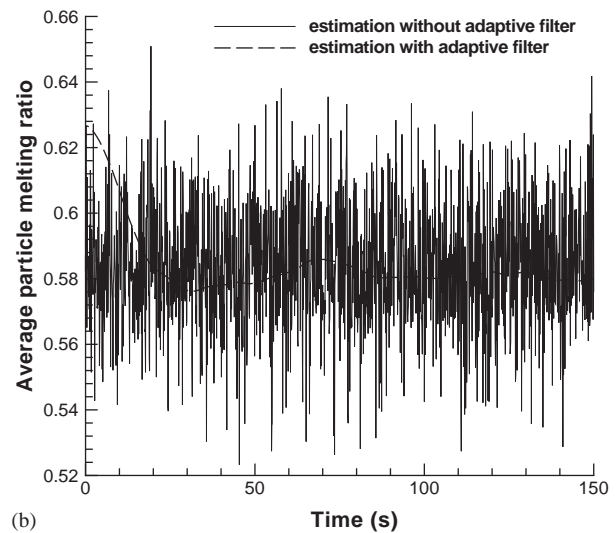
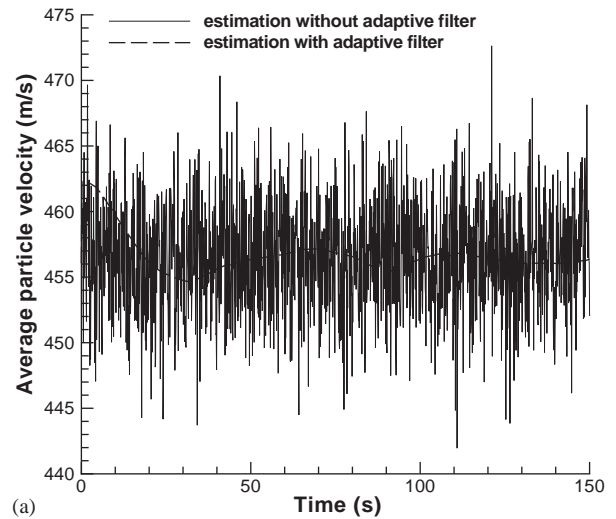


Fig. 4. Average particle velocity (a) and particle melting ratio (b) at the point of impact on the substrate under noise in the measurements of gas phase—simulation with and without adaptive filter.

average of particle velocity and degree of melting can be almost independently regulated by manipulating the pressure in the chamber and the equivalence ratio (fuel/oxygen ratio divided by its value at stoichiometric condition), respectively. To develop a feedback controller that can be readily implemented in practice, the manipulation of the combustion pressure and the equivalence ratio is realized by adjusting the flow rate of propylene,  $u_1(t)$ , oxygen,  $u_2(t)$ , and air  $u_3(t)$  to the process. Owing to the almost decoupled nature of the manipulated input/controlled output pairs, two proportional-integral controllers are used to regulate the process of the following form:

$$\begin{aligned} \dot{\zeta}_i &= y_{sp_i} - \hat{y}_i, \zeta_i(0) = 0, i = 1, 2, \\ u'_i &= K_{ci} \left[ (y_{sp_i} - \hat{y}_i) + \frac{1}{\tau_{ci}} \zeta_i \right] + u'_{0_i}, i = 1, 2, \\ \{u_1, u_2, u_3\} &= f(u'_1, u'_2, w), \end{aligned} \quad (17)$$

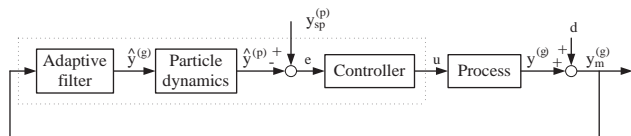


Fig. 5. Diagram of the closed-loop system under the proposed estimator/controller structure.

Table 1  
Estimator and controller parameters used in the closed-loop simulation

$K_s$	$K_0$	$K_{c1}$	$K_{c2}$	$\tau_{c1}$	$\tau_{c2}$
1.0	12.0	$10^{-3}$	$10^{-2}$	0.05	0.05

Table 2  
Operating conditions

Oxygen flow rate, <i>scfh</i>	578	Spray distance, <i>inch</i>	8
Propylene flow rate, <i>scfh</i>	176	$d_{10}$ , $\mu\text{m}$	5
Air flow rate, <i>scfh</i>	876	$d_{50}$ , $\mu\text{m}$	15
Nitrogen flow rate, <i>scfh</i>	28.5	$d_{90}$ , $\mu\text{m}$	45

where  $y_{sp_i}$  is the desired set-point value and  $\hat{y}_i$  is the value of the output obtained from the model-based estimator developed in the previous section ( $\hat{y}_1$  is the estimated volume-based average of particle velocity and  $\hat{y}_2$  is the estimated volume-based average of melting ratio).  $u'_1$  is the combustion pressure,  $u'_2$  is the equivalence ratio, and  $w$  is the air/oxygen ratio.  $K_{c_i}$  is the proportional gain and  $\tau_{c_i}$  is the integral time constant. The manipulated inputs, which are the fuel, oxygen, and air flow rates to the process, are then determined by solving the gas temperature and velocity equation. To keep the problem simple, a fixed  $w$  is used in the closed-loop simulation. It has been shown that the relationship between the gas temperature and the equivalence ratio is not monotonic. Beyond the optimal equivalence ratio (about 1.2), the gas temperature decreases as the equivalence ratio increases (Li et al., 2004a). Therefore,  $K_{c2}$  should be replaced by  $-K_{c2}$  if the initial equivalence ratio is beyond this value. The diagram of the closed-loop system under the developed estimator/control structure is shown in Fig. 5. The parameters used in the closed-loop simulation are given in Table 1. The readers may refer to Chiu and Christofides (1999, 2000), El-Farra et al. (2001) and the book (Christofides, 2002) for model-based control of particulate processes.

Several closed-loop simulation runs were performed to evaluate the ability of the proposed estimator/controller structure to: (a) regulate the average particle velocity and degree of melting at the point of impact on substrate to desired set-point values, and (b) attenuate the effect of disturbances on process operating conditions. In all the simulations, the adaptive filter is applied to the gas temperature and velocity measurements at all times and the process is operated under the conditions shown in Table 2 for 50 s, which is long enough for the controlled output estimates to converge to constant values. At time  $t = 50$  s, a change in the set-point value (or disturbance) is made and the controller is implemented. To evaluate the performance of the

feedback controller, the results of open-loop simulation in which the manipulated inputs are kept on constant values are also presented in the following figures. In the first simulation, we study the behavior of the closed-loop system in the presence of changes in the set-point. Specifically, at  $t = 50$  s, the set-point values of the average particle velocity and the average particle melting ratio change to 500 m/s and 0.65, respectively and the controller is implemented. Fig. 6 shows how the controlled outputs, manipulated inputs as well as the pressure and the equivalence ratio evolve in the case of requesting such changes in the set-point values. The controller drives the controlled outputs to the new set points in less than 1 min, which is much less than the typical time needed for coating deposition (this time is usually several tens of minutes). The simulation results show that the controller is quite effective in driving the controlled outputs to desired set-point values and validates the feasibility of implementing real-time feedback control on the HVOF thermal spray process.

Fig. 7 shows the profiles of the controlled outputs and the manipulated inputs as well as of the pressure and equivalence ratio in the presence of a 30% sudden increase in the spray distance occurring at  $t = 50$  s. Without control, the particle velocity drops and the melting ratio increases. This is because both the particle velocity and the degree of particle melting increase first and then decrease in the free jet. However, the optimal spray distance for maximum particle velocity and the one for maximum particle melting ratio are usually different. If the initial spray distance is in between these two locations, a change in the spray distance might have different effects on particle velocity and melting ratio. Under feedback control, the manipulated inputs drive the controlled outputs to their original steady state values in a very short time.

Fig. 8 shows the profiles of the controlled outputs and manipulated inputs as well as of the pressure and equivalence ratio in the presence of variation in the powder size. Variation in the powder size may occur in the practical environment due to possible nonuniform distribution of powders in the feedstock, which leads to time variant powder size distribution during delivery. In the simulation, it is assumed that the characteristic sizes describing particle size distribution,  $d_{10}$ ,  $d_{50}$ ,  $d_{90}$ , all increase gradually with time according to the expression  $d_p = d_{p0} [1 + 0.03(1 - e^{-t/100})]$ . When no control is used, both the velocity and the melting ratio of particles decrease with time, due to the increases in the particle momentum and thermal inertias. The resulting variation in the particle properties at the point of impact on the substrate is undesirable for the uniformity of the coating microstructure and properties. Under feedback control, both the particle velocity and the melting ratio fluctuate in a narrow range around the desired set-point values.

In conclusion, we have proposed an estimation scheme based on gas phase measurements and the momentum transfer and heat transfer equations to estimate the volume-based average of particle velocity and melting degree at the point

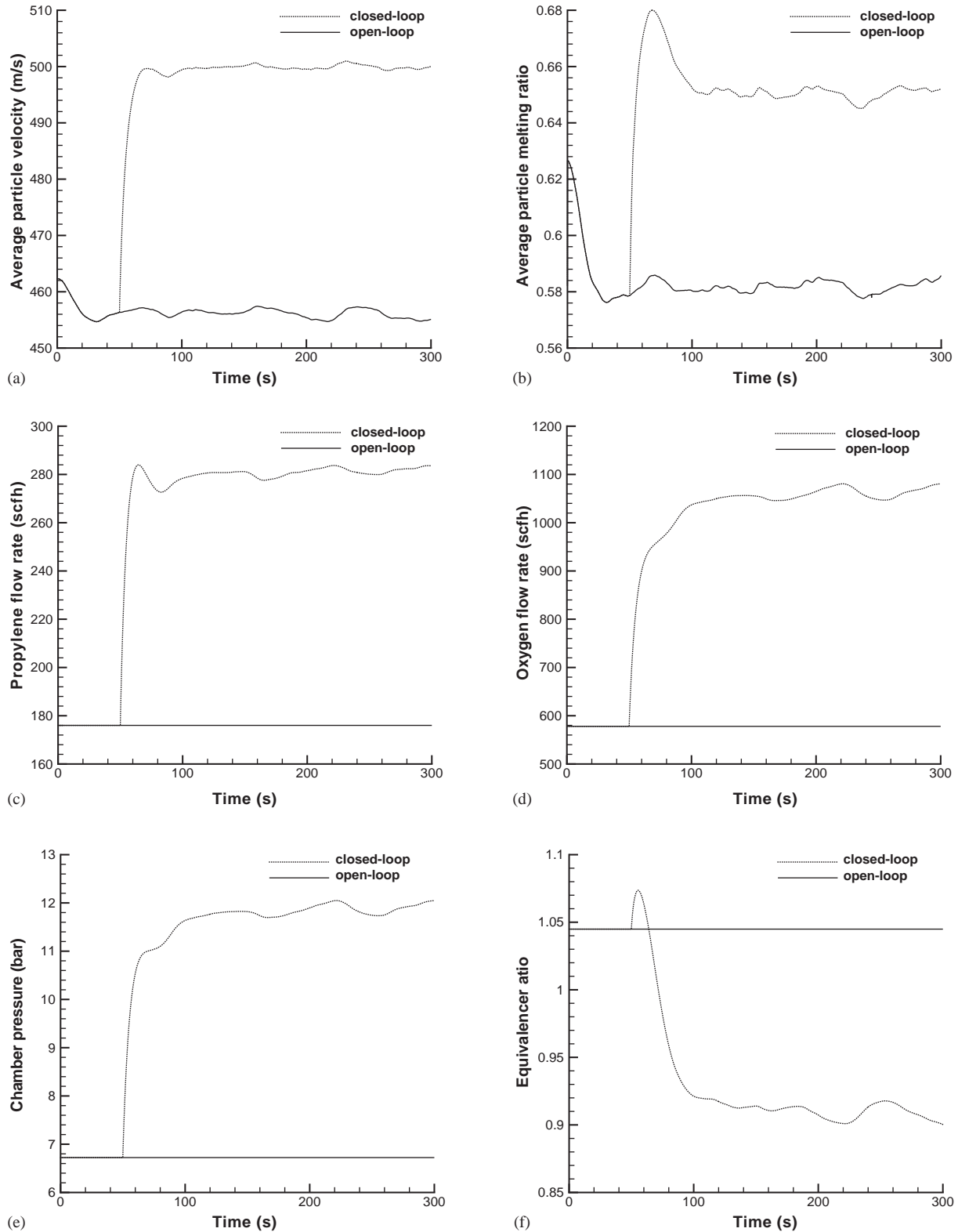


Fig. 6. (a–f) Profiles of controlled outputs (average particle velocity and average particle melting ratio), manipulated inputs (gas flow rates of propylene and oxygen), combustion pressure and equivalence ratio under the request of set-point change in the average particle velocity and average particle melting ratio.

of impact on the substrate. A feedback control system, which directly uses the estimation scheme, has been designed to regulate the volume-based average of the particle veloc-

ity and degree of melting by manipulating the inlet gas flow rates to the process. The proposed estimation/control structure has been applied to a fundamental model of the

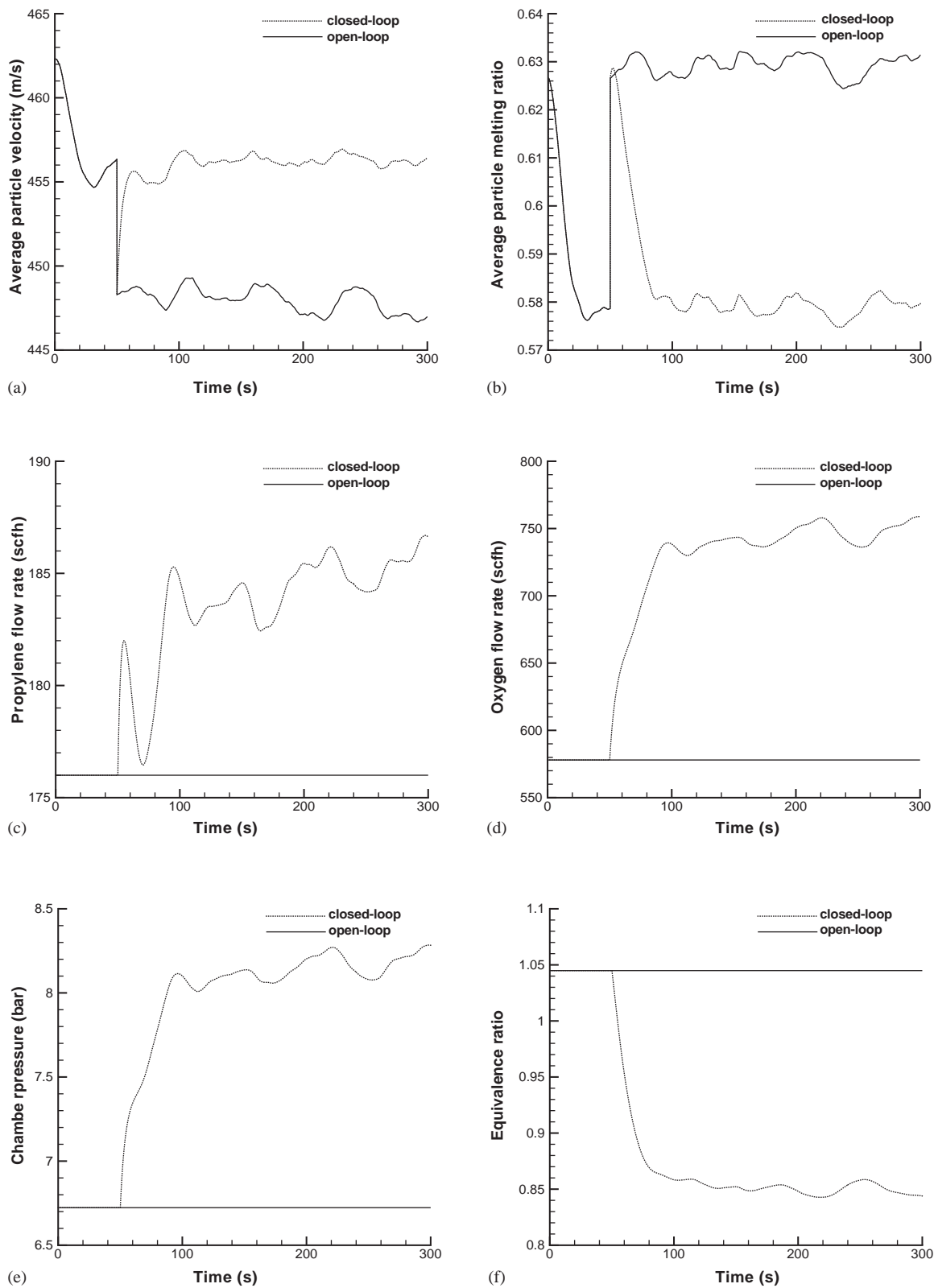


Fig. 7. (a–f) Profiles of controlled outputs (average particle velocity and average particle melting ratio), manipulated inputs (gas flow rates of propylene and oxygen), combustion pressure and equivalence ratio, in the presence of a 30% decrease in the spray distance.

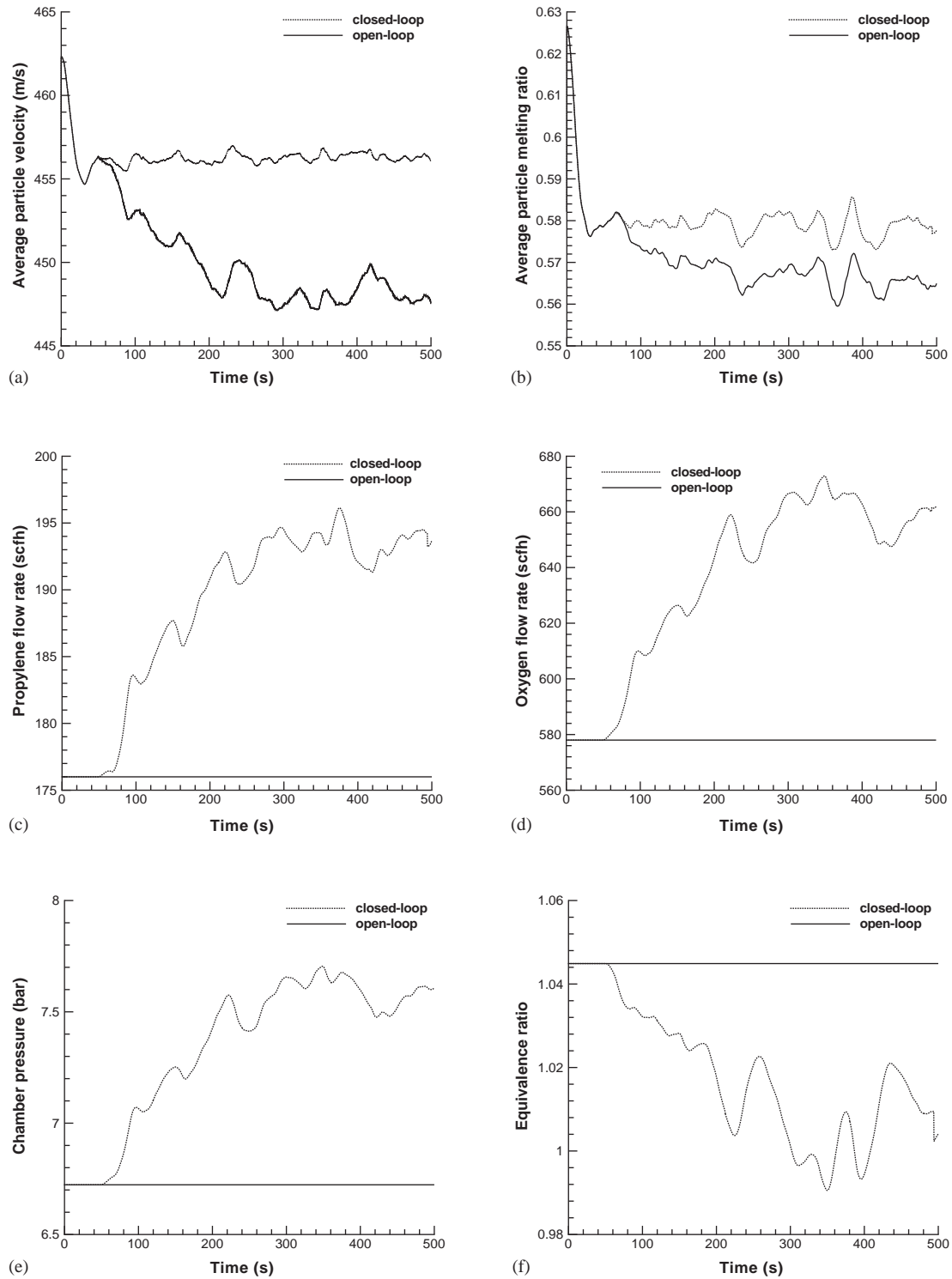


Fig. 8. (a–f) Profiles of controlled outputs (average particle velocity and average particle melting degree), manipulated inputs (gas flow rates of propylene and oxygen), combustion pressure and equivalence ratio, in the presence of 3% increase in the powder size.

industrial Diamond Jet hybrid HVOF thermal spray process and its performance and robustness properties have been successfully tested through simulations. Its feasibility to implement real-time feedback control on the HVOF process should be useful.

### Acknowledgements

Financial support from a 2001 Office of Naval Research Young Investigator Award, program manager Dr. Lawrence Kabacoff, is gratefully acknowledged.

## References

- Cheng, D., Xu, Q., Trapaga, G., Lavernia, E.J., 2001a. The effect of particle size and morphology on the in-flight behavior of particles during high-velocity oxyfuel thermal spraying. *Metallurgical and Materials Transactions B* 32, 525–535.
- Cheng, D., Xu, Q., Trapaga, G., Lavernia, E.J., 2001b. A numerical study of high-velocity oxygen fuel thermal spraying process. part I: gas phase dynamics. *Metallurgical and Materials Transactions A* 32, 1609–1620.
- Cheng, D., Trapaga, G., McKelliget, J.W., Lavernia, E.J., 2003. Mathematical modelling of high velocity oxygen fuel thermal spraying of nanocrystalline materials: an overview. *Modelling Simulation and Material Science Engineering* 11, R1–R31.
- Chiu, T., Christofides, P.D., 1999. Nonlinear control of particulate processes. *A.I.Ch.E. Journal* 45, 1279–1297.
- Chiu, T., Christofides, P.D., 2000. Robust control of particulate processes using uncertain population balances. *A.I.Ch.E. Journal* 46, 266–280.
- Christofides, P.D., 2002. *Model-Based Control of Particulate Processes*, Kluwer Academic Publishers, Particle Technology Series, Netherlands.
- El-Farra, N.H., Chiu, T., Christofides, P.D., 2001. Analysis and control of particulate processes with input constraints. *A.I.Ch.E. Journal* 47, 1849–1865.
- Fincke, J.R., Swank, W.D., Jeffrey, C.L., 1990. Simultaneous measurement of particle size, velocity and temperature in thermal plasmas. *IEEE Transaction on Plasma Science* 18, 948–957.
- Fincke, J.R., Haggard, D.C., Swank, W.D., 2001. Particle temperature measurement in the thermal spray process. *Journal of Thermal Spray Technology* 10, 255–266.
- Gordon, S., McBride, B.J., 1994. *Computer program for calculation of complex chemical equilibrium compositions and applications*, NASA Reference Publication 1311, Lewis Research Center, Cleveland, Ohio, USA.
- He, J., Ice, M., Lavernia, E.J., 2001. Particle melting behavior during high-velocity oxygen fuel thermal spraying. *Journal of Thermal Spray Technology* 10, 83–93.
- Hearley, J.A., Little, J.A., Sturgeon, A.J., 2000. The effect of spray parameters on the properties of high velocity oxy-fuel NiAl intermetallic coatings. *Surface Coating Technology* 123, 210–218.
- Kalani, A., Christofides, P.D., 1999. Nonlinear control of spatially-inhomogeneous aerosol processes. *Chemical Engineering Science* 54, 2669–2678.
- Kalani, A., Christofides, P.D., 2000. Modeling and control of a titania aerosol reactor. *Aerosol Science and Technology* 32, 369–391.
- Kalani, A., Christofides, P.D., 2002. Simulation, estimation and control of size distribution in aerosol processes with simultaneous reaction, nucleation, condensation and coagulation. *Computers and Chemical Engineering* 26, 1153–1169.
- Knight, R., Smith, R.W., Xiao, Z., 1994. Particle velocity measurements in HVOF and APS systems. In: *Thermal Spray Industrial Applications, Proceedings of the Seventh National Thermal Spray Conference*, pp. 331–336.
- Li, M., Christofides, P.D., 2003. Modeling and analysis of HVOF thermal spray process accounting for powder size distribution. *Chemical Engineering Science* 58, 849–857.
- Li, M., Christofides, P.D., 2004. Feedback control of HVOF thermal spray process accounting for powder size distribution. *Journal of Thermal Spray Technology* 13, 108–120.
- Li, M., Christofides, P.D., 2004. Multiscale modeling and analysis of an industrial HVOF thermal spray process. *Chemical Engineering Science*, submitted.
- Li, M., Shi, D., Christofides, P.D., 2004a. Diamond jet hybrid HVOF thermal spray: gas-phase and particle behavior modeling and feedback control design. *Industrial and Engineering Chemistry Research* 43, 3632–3652.
- Li, M., Shi, D., Christofides, P.D., 2004b. Modeling and control of HVOF thermal spray processing of WC-Co coatings. *Powder Technology*, accepted.
- Lugscheider, E., Herbst, C., Zhao, L., 1998. Parameter studies on high-velocity oxy-fuel spraying of MCrAlY coatings. *Surface Coating Technology* 108–109, 16–23.
- Moreau, C., Leblanc, L., 2001. Optimization and process control for high performance thermal spray coatings. *Key Engineering Materials* 197, 27–57.
- Press, W.H., Teukolsky, S.A., Vetterling, W.T., Flannery, B.P., 1997. *Numerical Recipes in C++: The Art of Scientific Computing*, second ed. Cambridge University Press, NY, USA.
- Roberson, J.A., Crowe, C.T., 1997. *Engineering Fluid Dynamics*, sixth ed. Wiley, NY, USA.
- Shi, D., Li, M., Christofides, P.D., 2004. Diamond jet hybrid HVOF thermal spray: rule-based modeling of coating microstructure. *Industrial and Engineering Chemistry Research* 43, 3653–3665.
- Sobolev, V.V., Guilemany, J.M., Garmier, J.C., Calero, J.A., 1994. Modelling of particle movement and thermal behavior during high velocity oxy-fuel spraying. *Surface Coating Technology* 63, 181–187.
- Swank, W.D., Fincke, J.R., Haggard, D.C., Irons, G., 1994. HVOF gas flow field characteristics. In: *Proceedings of the Seventh National Thermal Spray Conference*, pp. 313–318.
- Zhang, D., Harris, S.J., McCartney, D.G., 2003. Microstructure formation and corrosion behaviour in HVOF-sprayed Inconel 625 coatings. *Materials Science Engineering A* 344, 45–56.